

Gravitational Wave Background from Extragalactic Double WhiteDwarfs for LISA

Cosmological Population Modeling of DWD with COSMIC

Guillaume Boileau, Tristan Bruel, Astrid Lamberts and Nelson Christensen

LISA Astrophysics Working Group Meeting
5-7 November 2024

Context : The Stochastic Gravitational Wave Background (SGWB) for LISA

Stochastic Background : Superposition of a large number of independent sources (unresolved sources):

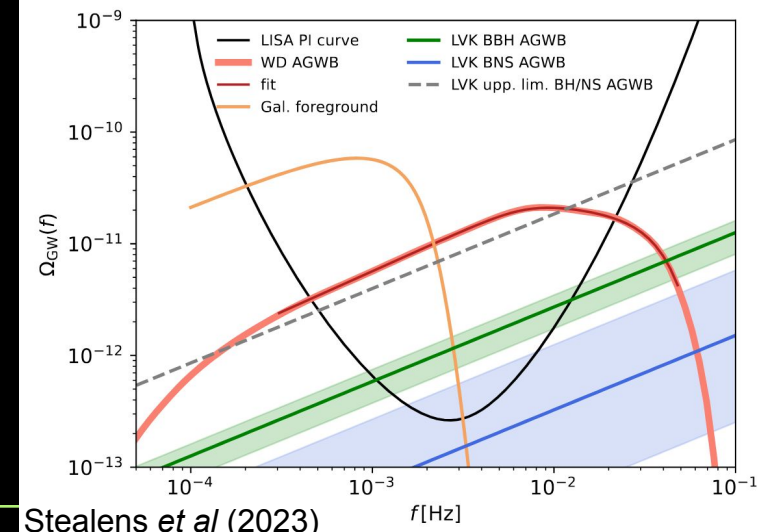
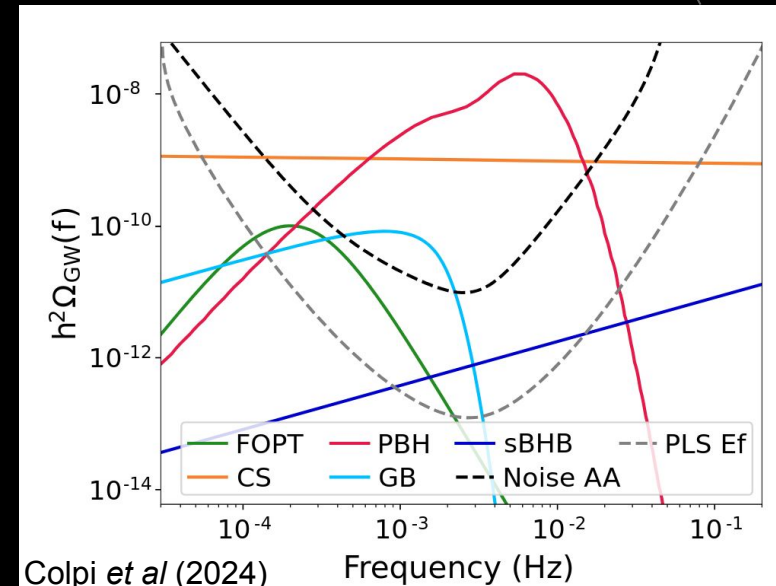
$$\Omega_{GW}(f) = \frac{1}{\rho_c} \frac{d\rho_{GW}}{d \ln f}$$

Galactic and Cosmological SGWB Sources:

- **Galactic SGWB:** Primarily generated by unresolved compact binaries (e.g., double white dwarfs), creating a foreground. Robson *et al* (2019), Boileau *et al* (2021)
- **Astrophysical SGWB :** Binary Black Holes & Neutron Stars (LIGO/Virgo Band) (Abbott *et al.* (2019, 2021))
- **Cosmological SGWB:** Originates from the early Universe, with a weaker signal often obscured by astrophysical noise Boileau *et al* (2022, 2023).

New source Extra-Galactics DWD :

- First estimated from Farmer and Phinney (2003):
- Recent work on Stealens and Nelemans (2023) and Hofman and Nelemans (2024).



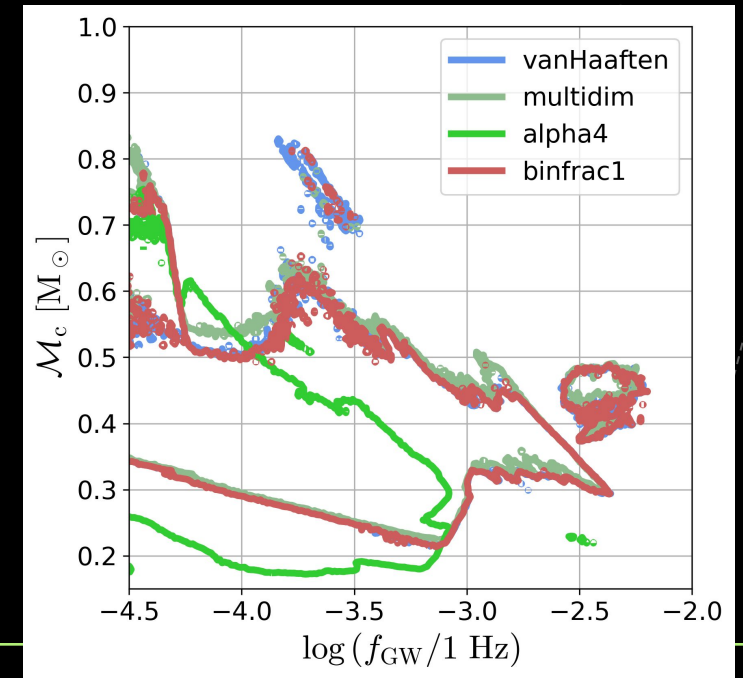
Method: Overview of Double White Dwarf Population Synthesis

- **Key population synthesis properties COSMIC Breivik et al (2020):**
 - **Common-Envelope (CE):** Governed by parameters α (energy efficiency) and λ (binding energy).
 - **Default Model Setup:** Uses Kroupa IMF for star masses, binary formation rates, and distributions for orbital separation and eccentricity (Sana et al).
 - **Covers a range of metallicities for realistic stellar populations** (25 values in [1e-04, 0.03] log selection).
- **DWD Formation Efficiency:**
 - **Default Model:** Baseline formation efficiency for solar metallicity.
 - **Alternative Models:**
 - **fb1:** Assumes all stars are binaries, boosting DWD count.
 - **Multidim:** Uses correlated distributions for initial binary properties. Moe et al (2017)
 - **α 4:** Increased CE efficiency ($\alpha = 4$) enhances DWD production.
- **GW Frequency Distribution:**
 - Most DWDs fall within the LISA detection band at formation, grouped by WD composition (He, CO, ONe).
 - DWD formation efficiency increases with adjustments in CE efficiency, binary fraction, and multidimensional sampling.

Model	$M_{SF} [M_{\odot}]$	N_{DWDs}	$\eta [M_{\odot}^{-1}]$
default	8.5×10^7	2.4×10^5	2.9×10^{-3}
fb1	4.6×10^7	1.9×10^5	4.1×10^{-3}
multidim	4.3×10^7	1.8×10^5	4.2×10^{-3}
$\alpha 4$	3.7×10^7	4.5×10^5	1.2×10^{-2}

$$\eta(Z) = \frac{N_{DWDs}(Z)}{M_{SF}(Z)}$$

Population Synthesis Efficiency



Method: Orbital Dynamic Evolution in Double White Dwarf Systems

Frequency Transition Time:

- The time required to evolve between two frequencies $f_1 \rightarrow f_2$ is:
$$\Delta T(f_1, f_2) = \frac{3}{8K} \left(f_1^{-\frac{8}{3}} - f_2^{-\frac{8}{3}} \right)$$

Stopping Criterion with Roche Lobe:

- Roche lobe:**

$$R_{L2}(q, a) = \frac{a \cdot 0.49q^{2/3}}{0.6q^{2/3} + \log(1 + q^{1/3})}$$

- The orbital evolution stops when the Roche lobe boundary is reached, as further dynamical evolution is constrained.

Gravitational Wave Emission from Binary Systems:

- Gravitational wave luminosity for circular orbits:
$$L_{\text{circ}}(f_{e,\text{circ}}) = \frac{32\pi^{10/3} G^{7/3} M_c^{10/3}}{5 c^5} f_{e,\text{circ}}^{10/3}$$
- No eccentricity from COSMIC results, negligible from Farmer *et al* (2003) conclusion

Method : Computing the Background Energy Density Spectrum for DWD Systems

Integral Discretization and Bin Setup:

- Redshift z divided into 20 bins over 0 to 8 for a linear progression in lookback time.
- Frequency divided into 17 bins from 0.05 mHz to 70 mHz.

Energy Density Spectrum: $\Omega_i(f_r, z) = \frac{f_r F_{f_r}(f_r)}{\rho_c c^3}$

Luminosity Sum and Number Density:

- Total luminosity from sources at redshift horizon: $\ell_{f_e}(T_i) = \sum_{k,j} N_{k,j}(z_i) L_{e,k,j}(f_e)$
- Number density of binaries:

$$N_{k,j}(z_i) = \Delta t(k, bin) \text{SFR}(z) \mathcal{P}_k$$

- **Final Spectrum Calculations:**
- Integrate received flux per frequency bin: $F_{f_{f_1} \rightarrow f_{f_2}} = \sum_i \int_{f_{r_1}(1+z_i)}^{f_{r_2}(1+z_i)} \frac{\ell_{f_e}}{(1+z_i)^2} \frac{df_e}{df_r} df_e \Delta\chi(z_i)$

- Sum specific luminosity density over population synthesis sources.
- Total energy density spectrum per metallicity and final spectrum: $\Omega_{\text{bin}} = \sum_Z \Omega_{\text{per}Z}$

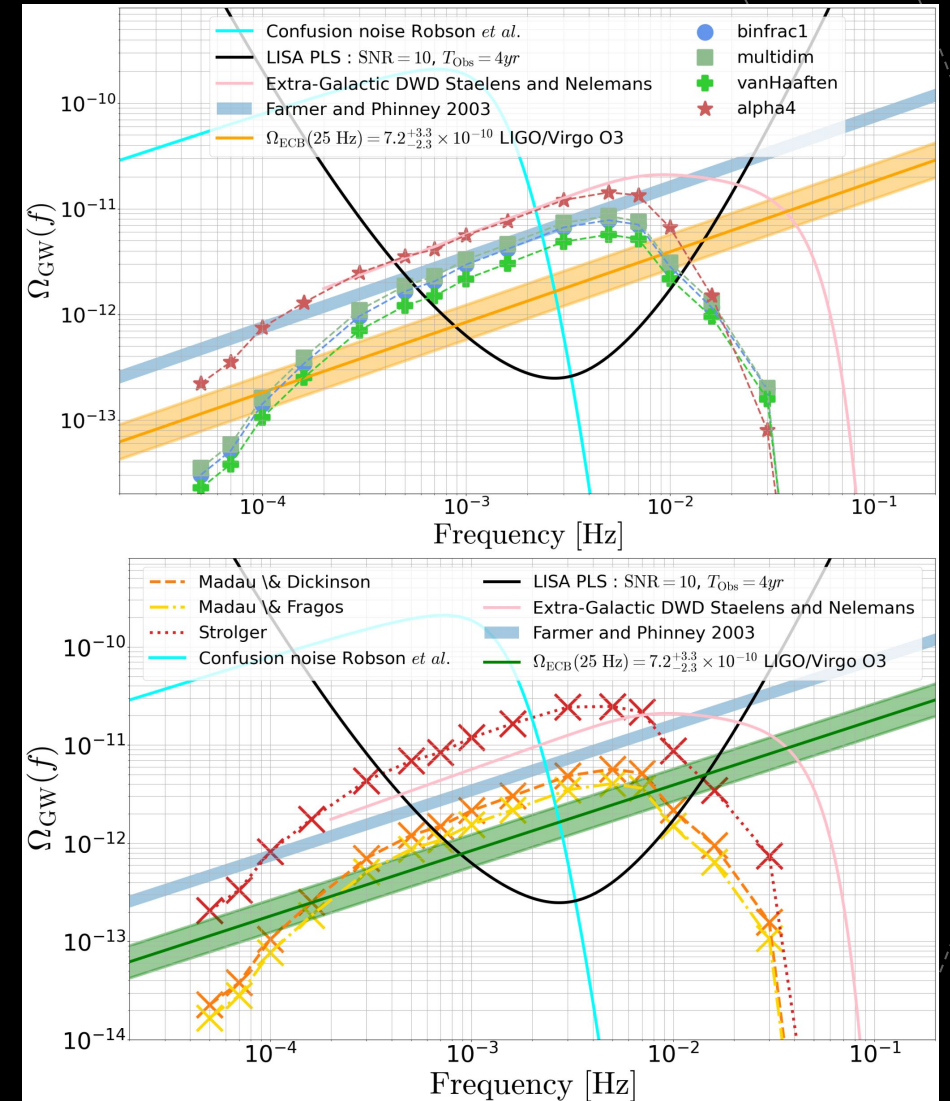
Results : Validation and Comparison with Literature

Gravitational Wave Background Analysis:

- Good Amplitude recovery from different hypothesis on binary evolution synthesis and SFR
- **Observed Shift:** The observed frequency break remains consistent across models; however, discrepancies may arise from inaccuracies in the radii of higg-mass binaries derived from COSMIC.
- Analysis includes:
 - SFR models Strolger et al. (2004), Madau & Dickinson (2014), Madau & Fragos (2017),
 - SFR variation over redshift and metallicity Neijssel et al (2019)
 - Metallicity bins from $Z = 0.03$ to $Z=0.0001$
 - Redshift range $0 \leq z \leq 8$

Observations:

- **Star Formation Rate :** Choice of SFR directly affects binary populations and AGWB predictions.
- **Stellar Synthesis Parameters:** Different synthesis assumptions in binary evolution can lead to varied AGWB profiles.



Results : Stellar Evolution and Assumptions Impact on DWD Populations in COSMIC

Influence of Redshift Range:

- AGWB mostly shaped by sources with $z < 2$
- High-frequency signals are primarily from sources at $z \leq 0.5$ and $z \leq 0.043$ (nearby universe).

Stellar Synthesis Models:

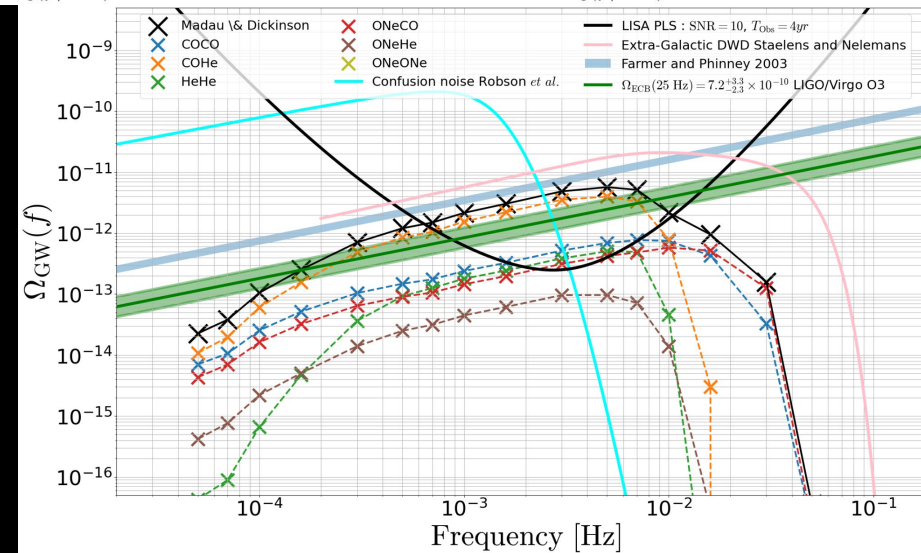
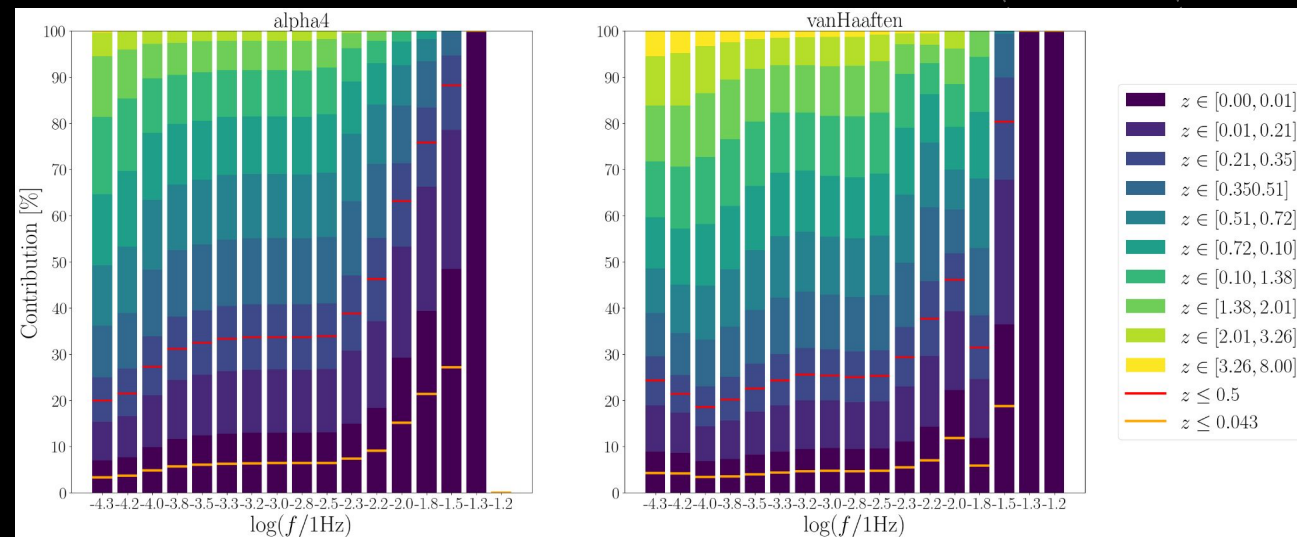
- Comparison of different stellar evolution assumptions in COSMIC, focusing on $\alpha 4$ and **default** models.
- Distribution of frequency vs. redshift shows differences at higher LISA frequencies, due to the rarity of high-frequency DWD mergers..

Population Characteristics:

- **ONeONE Binaries:** Minimal contribution due to rarity
- **HeHe Binaries:** Slow evolution contributes mostly at lower redshifts.

Model Sensitivity:

- Spectral differences reflect choices in stellar evolution (e.g., common-envelope efficiency α).
- Lower α values reduce the AGWB amplitude but do not shift the frequency break.



Results : Potential Anisotropies in the AGWB

Cumulative AGWB Contribution by Redshift:

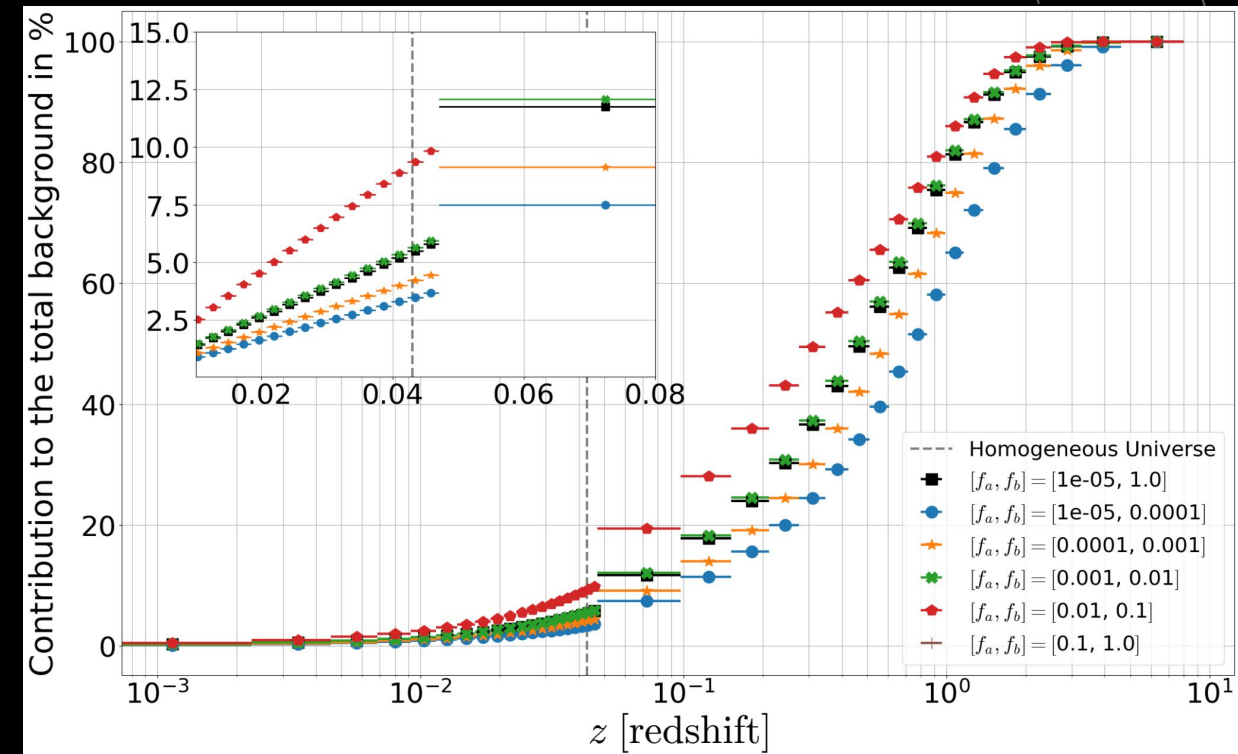
- Analysis based on Mauda and Dickinson (2014) SFR model and *default* model synthesis.
- Redshift range $z \approx 0.043$ marks the homogeneous universe limit (200 Mpc); anisotropies are more prominent at low redshifts.

Frequency Dependence:

- High-frequency bins, especially in the range [0.01, 0.1] Hz, contribute more to AGWB anisotropies.
- Signals from closer redshift shells (e.g., NeONeO binaries) introduce slight anisotropies due to their localized origins.

Isotropy vs. Anisotropy:

- Lower frequency sources, found at higher redshifts, create a more isotropic background.
- Minor anisotropies ($\sim 7\%$) are observed but are negligible when considering the isotropic component of the AGWB.



Discussion and Conclusions

Influence of Model Choices:

- **Star Formation Rate** : Choice of SFR directly affects binary AGWB predictions.
- **Termination Criterion**: Using Roche lobe contact as a threshold is conservative. A less strict approach could alter orbital dynamics and shift the frequency break. Toubiana *et al* (2024)
- **Stellar Synthesis Parameters**: Different synthesis assumptions in binary evolution can lead to varied AGWB profiles.

Measurement and Interpretation:

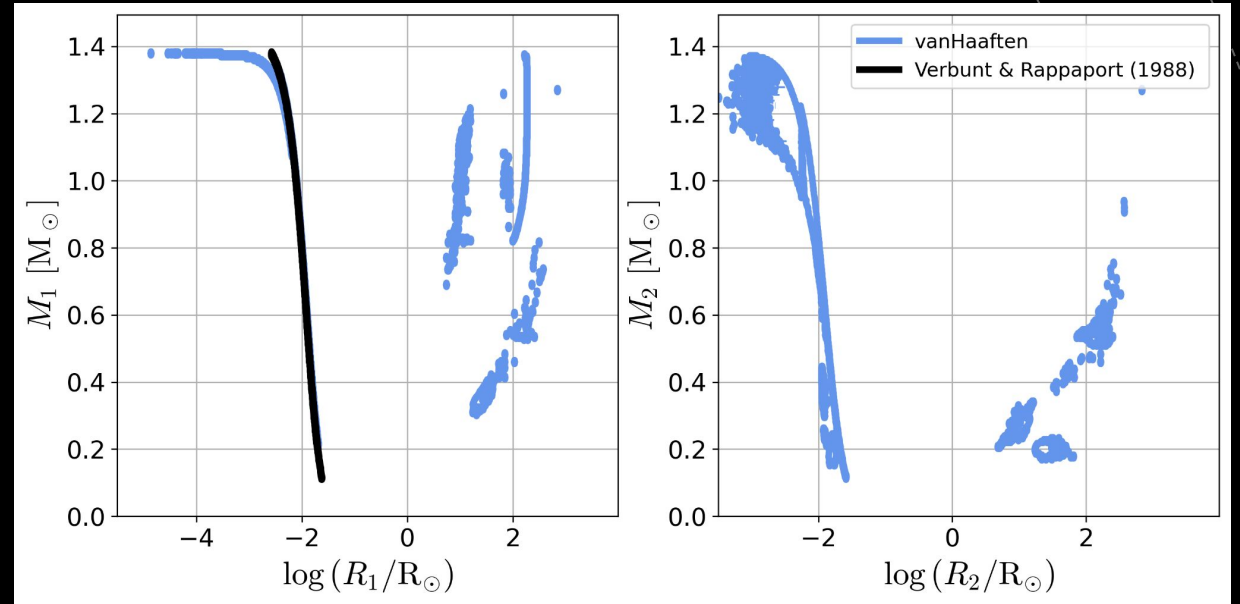
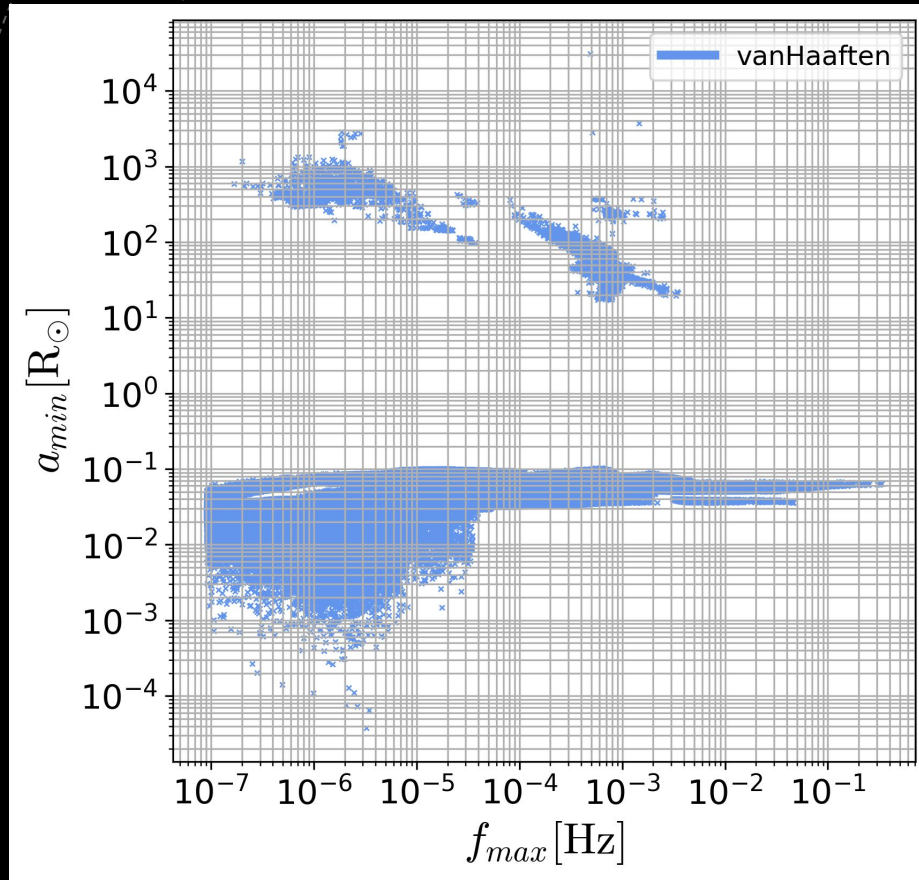
- **Stochastic vs. Resolved Sources**: AGWB estimation presents challenges in separating stochastic signals from resolved sources. This complicates LISA data interpretation.
- **Population Generation Algorithm**: The selected algorithm impacts the generated population dynamics, influencing AGWB characteristics.

Implications for Future Studies:

- **Simulation Enhancements**: Adding refined AGWB components and exploring varied algorithms (stellar synthesis) could provide more comprehensive insights for LISA simulations.
- **Low Anisotropy Impact**: Minimal AGWB anisotropy suggests limited utility in mitigating AGWB's influence on other gravitational wave measurements.

Thanks

Back-up Slide : Frequency Break



Verbunt and Rappaport (1988)

$$\frac{R}{R_{\odot}} = 0.0114 \left[\left(\frac{M}{M_{\text{Ch}}} \right)^{-2/3} - \left(\frac{M}{M_{\text{Ch}}} \right)^{2/3} \right]^{1/2} \left[1 + 3.5 \left(\frac{M}{M_{\text{p}}} \right)^{-2/3} + \left(\frac{M}{M_{\text{p}}} \right)^{-1} \right]^{-2/3}$$

$M_{\text{Ch}} = 1.4M_{\odot}, M_{\text{p}} = 5.7 \times 10^{-4}M_{\odot}$

$$a_{\text{min}} = \max \left[R_1 \frac{0.6q^{-2/3} + \log(1 + q^{-1/3})}{0.49q^{-2/3}}, R_2 \frac{0.6q^{2/3} + \log(1 + q^{1/3})}{0.49q^{2/3}} \right]$$

$$q = \frac{M_2}{M_1}$$